ORNL/SPR-2019/1129

Progress Report on Modified Burst Testing and Alternative Test Methods

Nuclear Technology Research and Development

Approved for Public Release

Prepared for
US Department of Energy
Advanced Fuels Campaign
M. N. Cinbiz
B. Garrison
R. R. Lowden
R. Sitterson
K. Linton
Oak Ridge National Laboratory

April 2019
M4FT - 19OR020204081

SUMMARY

Performance of accident-tolerant fuel and cladding (ATF) candidates must be assessed during the pellet-cladding mechanical interaction (PCMI) phase of a design-basis reactivity-initiated accident (RIA). We describe fiscal year 2019 research activities for the development of separate-effects testing for ATF cladding candidate iron-chromium-aluminum (FeCrAl) tube specimens under loading conditions comparable to PCMI.

The first section of this report provides modified burst test (MBT) results for unirradiated FeCrAl tubes at various pressurization rates and an RIA-relevant temperature (275°C). The failure strain of FeCrAl was observed and calculated using a high-speed digital-image-correlation technique developed recently under the US Department of Energy's Advanced Fuels Campaign.

To overcome the complexities of performing MBTs on irradiated samples in a hot-cell environment, a plane-strain tension (PST) test was proposed as an alternative method for PCMI testing. The relevance of the PST test as an alternative to an MBT for irradiated specimens was elucidated based on using the data available in the literature. We designed a hot-cell compatible PST fixture and a specific holder for PST hot-cell specimen machining.

INTENTIONALLY BLANK

CONTENTS

FIGURES

TABLES

ACRONYMS

ATF	accident-tolerant fuel
DIC	digital-image-correlation
FeCrAl	iron-chromium-aluminum (alloy)
IFEL	Irradiated Fuel Examination Laboratory
LWR	light-water reactor
MBT	modified burst test
ORNL	Oak Ridge National Laboratory
PCMI	pellet-cladding mechanical interaction
PST	plane-strain tension
RIA	reactivity-initiated accident

ACKNOWLEDGMENTS

This work was supported by the US Department of Energy Office of Nuclear Energy Advanced Fuels Campaign. The authors thank Dr. Daniel M. Wachs of Idaho National Laboratory for his oversight of this area.

PROGRESS REPORT ON MODIFIED BURST TESTING AND ALTERNATIVE TEST METHODOLOGIES

1. INTRODUCTION

Cladding candidates for accident-tolerant fuel (ATF) must preserve or improve the current reactor safety characteristics of light-water reactors (LWRs) during a postulated reactivity-initiated accident (RIA). RIAs may occur as a result of the ejection of the control rods from the nuclear reactor's core, which causes a sudden increase of the fission-rate density in nuclear fuel. The energy associated with the fission-rate density is deposited in the fuel as well. The temperature of the fuel rapidly increases, and the fuel experiences isotropic thermal expansion. As a result of the increased temperature, the negative temperature feedback effect cuts off the fission events. If the fuel-cladding gap is closed or closes during an RIA, the expansion of fuel induces mechanical strain on the cladding. This is referred to as the pellet-cladding mechanical interaction (PCMI) phase of RIA. These events occur within 10–100 ms. If the mechanical strain on the cladding is sufficient, the cladding may rupture. Therefore, assessment of the mechanical behavior of ATF cladding candidates during the PCMI phase of RIA is vital for the safety of LWRs.

RIAs impose special mechanical loading conditions on cladding tubes. Cladding tubes are expected to be under a multiaxial (minor-to-major stress ratio (σ_2/σ_1) is close to 1) and strain-driven loading with strain-rates of 1–5 s^{-1}. Therefore, mechanical behavior of the irradiated and unirradiated cladding has been extensively studied with integral and separate-effects tests [1–4]. While integral tests are important for establishment of acceptance criteria for ATF candidates for RIAs, separate-effects testing can inform both integral testing parameters and modeling tools for the candidate ATF claddings.

In our earlier report, we investigated the mechanical behavior of ATF cladding candidates for PCMI performance using a pulse-controlled modified burst test (MBT) and a novel digital-image-correlation (DIC) approach [5]. Modified burst testing can simulate the strain-driven conditions at RIA-relevant timescales. However, implementation of MBTs in a hot-cell environment needs extensive research. Therefore, we proposed the plane-strain tension (PST) test as an MBT alternative in the hot-cell environment. In this report, we present the MBT results for nuclear-grade iron-chromium-aluminum (FeCrAl) tubes and related PST test developments, including the relation between modified burst and plane-strain tension testing in hot-cell environments, specimen machining capability, and design of hot-cell-compatible fixtures for a universal mechanical loading frame.

2. MODIFIED BURST TEST RESULTS FOR NUCLEAR-GRADE FeCrAl

As-drawn nuclear-grade FeCrAl alloy (C26M) samples were subjected to an MBT at 275°C. Samples had a nominal outer diameter of 9.48 mm and a wall thickness of 0.39 mm. Table 1 shows the nominal value of the alloying elements of C26M.

Table 1 Alloying elements of the nuclear-grade FeCrAl (C26M). Iron is the balance.

	Cr	Al	Mo	Si	Yt
wt %	12	6.22	1.98	0.2	0.03

Samples were subjected to various pressurization rates to investigate the effect of the strain rate on the deformation of these samples. A telecentric lens and high-speed camera system, described in an earlier ORNL technical report [5], were used with a mirror setup for 360° observation of the deformation behavior of the sample (see Figure 1). Mechanical strains were determined using a DIC technique. The subset size was 85 × 85 px^2. The DIC-calculated failure strains, shown in Table 2, were calculated to be in the 2.7%–4.2% range. Current results did not indicate a strong strain-rate effect on the failure strain of the specimens.

Table 2 MBT results for FeCrAl (C26M) tubes

Sample	Core-pin speed [in./s (m/s)]	Pressurization rate [GPa/s]	Failure strain [%]
1 (FeCrAl-MBT-13)	5 (0.127)	1.5	2.91
2 (FeCrAl-MBT-11)	10 (0.254)	3.2	2.67
3 (FeCrAl-MBT-9)	25 (0.635)	6.4	3.44
4 (FeCrAl-MBT-10)	50 (1.270)	9.1	4.19
5 (FeCrAl-MBT-3)	80 (2.032)	9.4	3.90

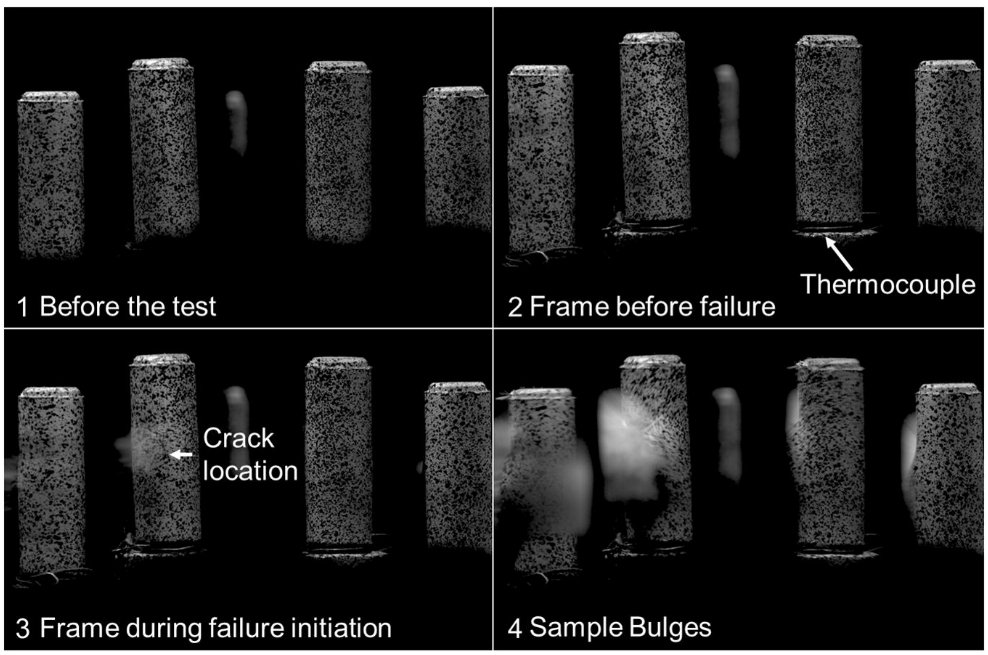

Figure 1 Deformation of the FeCrAl (C26M) sample tested at a core-pin speed of 25 in/s (0.635 m/s). Thermocouples were mechanically attached.

3. THE PLANE-STRAIN TENSION TEST FOR PCMI TESTS

PST was initially developed to assess the mechanical response of zirconium-based claddings to RIA-like conditions [3,6]. The schematic of the PST test is shown in Figure 2a. The sample is pulled apart by the motion of two cylindrical mandrels. The specimen has a double-edge notched geometry (only on one side), which imposes near plane-strain loading conditions (see Figure 2b). To induce a strain-driven effect, the specimen's gauge section is oriented perpendicular to the loading axis. The loading condition imposes a multiaxial stress state at the gauge center of the specimen where the stress biaxiality (σ_2/σ_1) is ~ 0.5 (PST or internal pressurization). At the notch roots, the σ_2/σ_1 becomes 0 (uniaxial tension) [3,6]. This was also confirmed by finite element analysis (FEA) of the ideal PST test as depicted in Figure 3. The biaxiality ratio at the gauge center is calculated as 0 and 0.48 at notch roots and gauge center, respectively.

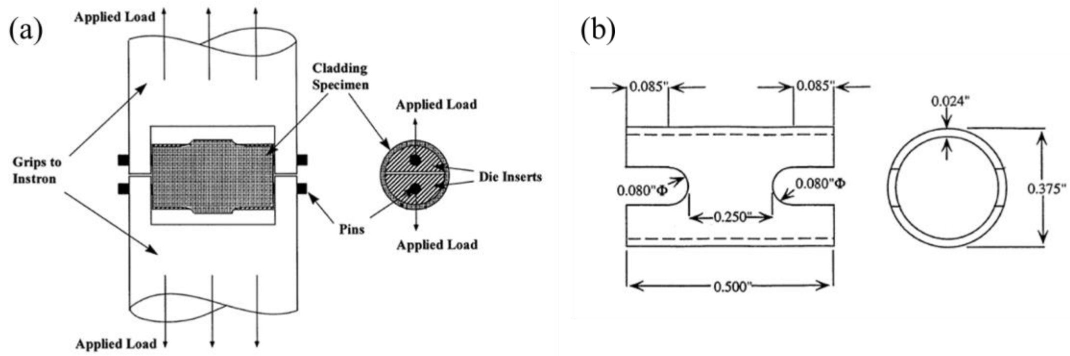

Figure 2 (a) Schematics of the original plane-strain tension test and (b) the specimen geometry. Note the gauge section is on the top of the mandrel where the loading direction is perpendicular to the gauge section [6].

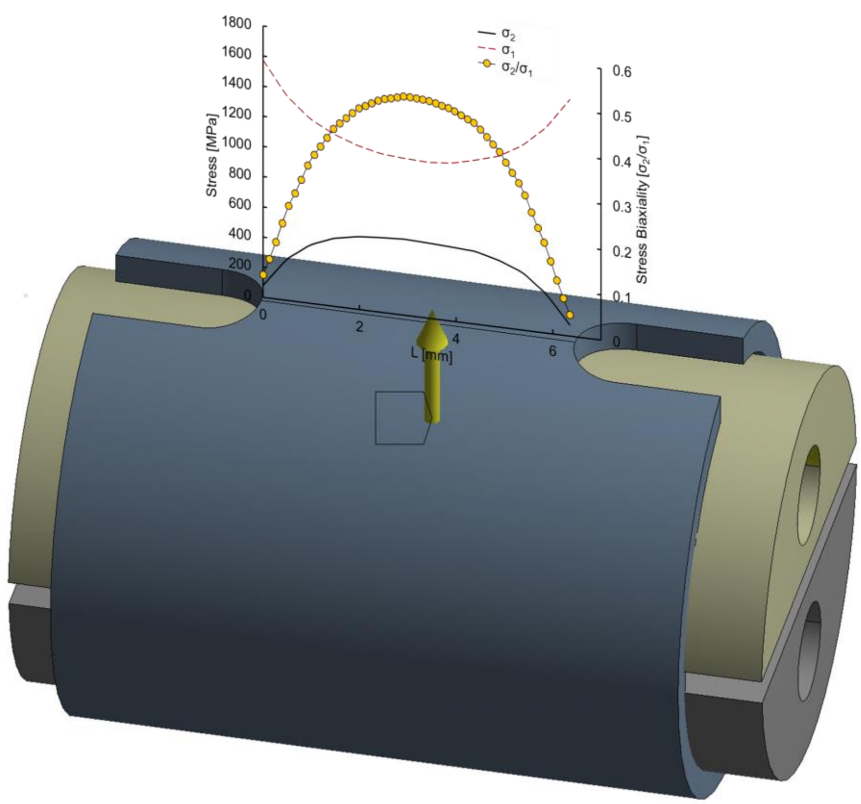

Figure 3 The stress and stress state distribution along the gauge section of the PST sample. ANSYS Workbench 17.1 is used for the finite element analysis of the PST test. FeCrAl properties are used to describe the material's constitutive relations [8]. The curve with yellow dots shows the stress biaxiality. The red and black curves stand for the major (σ_1) and minor (σ_2) stresses, respectively.

Figure 4 shows the failure strain of the hydrogen-charged zirconium-based cladding tubes as a function of hydrogen content for various tests [9]. The ring tension and expansion-due-to-compression tests have a similar loading path, which is uniaxial tension, and the failure strains of both tests are determined similarly [10,11]. On the other hand, the MBT and PST test are expected to have a near plane-strain tension loading path, and the resultant failure strains are similar as well [9]. Thus, the comparison of both test results supports the assertion that PST is a feasible alternative for testing irradiated tube geometries in a hot-cell environment.

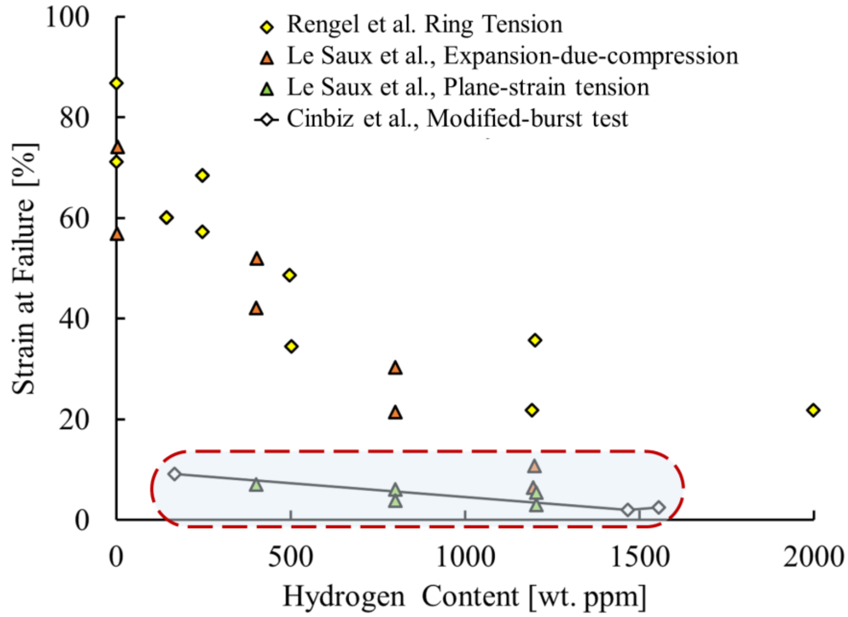

Figure 4 Comparison of failure strains of various tube tests. Ring-tension and expansion-due-to-compression tests have the same loading paths [10,11]. The loading paths of the PST test [11] and MBT [9] are expected to be similar.

Machining of the PST test specimen geometry is performed using a holder made of an aluminum alloy, as shown in Figure 5. A mill, which is the mock-up of one located in the Irradiated Fuels Examination Laboratory (IFEL, a hot-cell facility at ORNL), is used for machining the specimen notch from a standard thin-wall tube geometry. The tube specimen is pushed through the hole of the aluminum holder. The end mill is aligned perpendicular to the outer surface of the tube and machines the notch. The second notch is machined by rotating the aluminum part and repeating the cut.

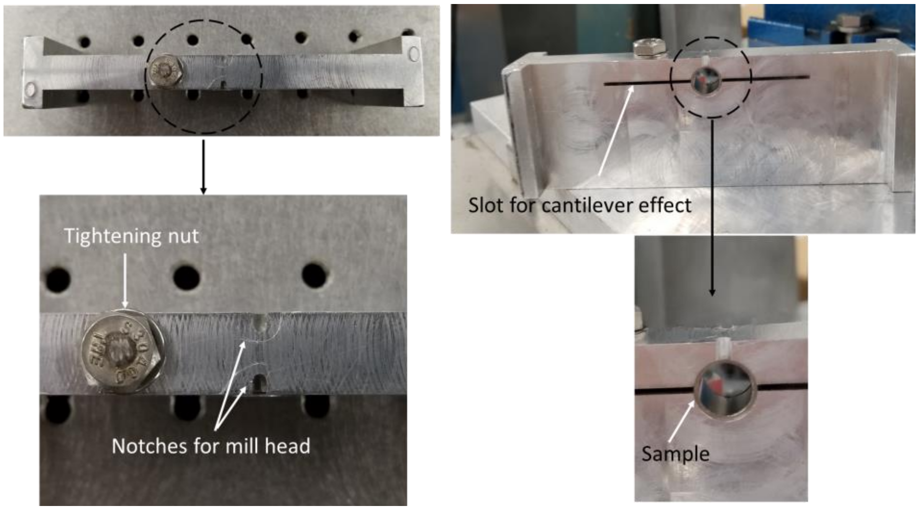

Figure 5 Holder for milling a double-edge notched specimen for PST tests.

We have performed a PST test of a FeCrAl sample using a pin-loading fixture geometry; however, the fixture would be very difficult to implement in a hot-cell environment to ensure the sample is centered and does not rotate. A new PST test fixture, shown in Figure 6, was designed for the Instron machine in IFEL. Use of slots and single-piece mandrels eliminated centering problems. For the sample rotation, the upper mandrel included two alignment beads having the same notch geometry as the PST sample.

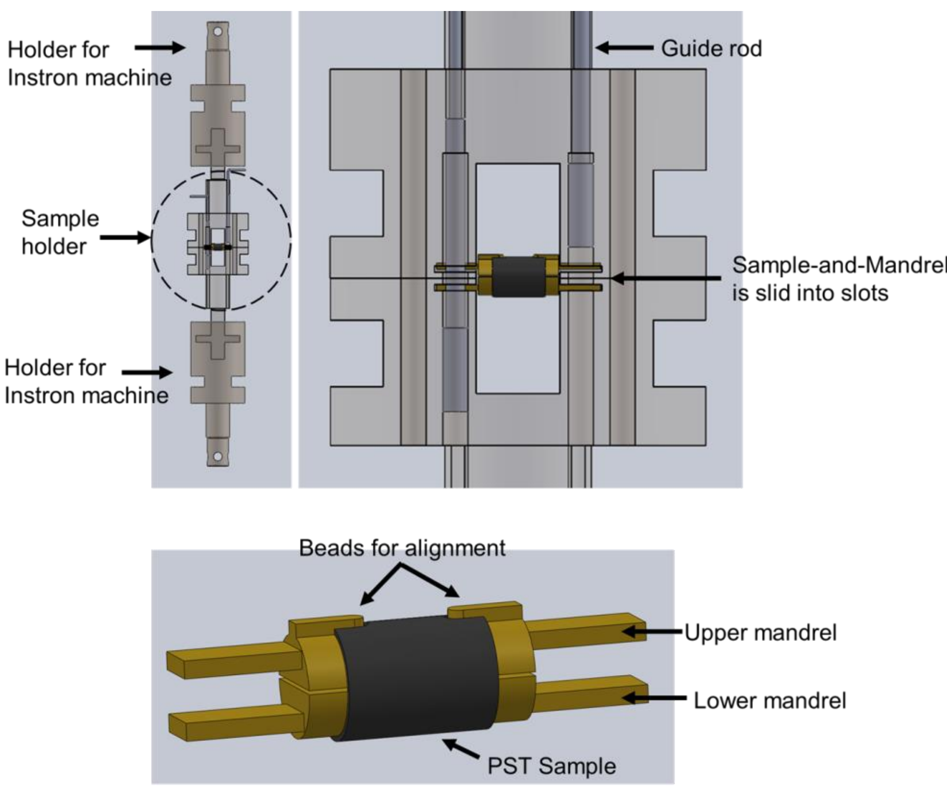

Figure 6 Schematics of the fixtures for the PST test.

4. SUMMARY AND FUTURE WORK

This report describes the mechanical response of nuclear-grade FeCrAl (C26M) under PCMI-like deformation and the development of PST tests. Mechanical tests were performed using the pulse-controlled MBT instrument and the high-speed optical metrology developed recently for the Advanced Fuels Campaign. Failure strains of nuclear-grade FeCrAl (C26M) were determined to be in the 2.7%–4% range. MBT data showed that the strain-rate effect on the failure strain was weak for this specific alloy.

The current MBT instrument and the 360°-DIC provide exceptional capabilities to assess the PCMI performance of unirradiated cladding. However, implementation in the hot-cell environment is not practical. Therefore, PST testing is being pursed as an alternative for PCMI testing of irradiated materials. The recent installation of a universal Instron mechanical frame facilitates PST testing of irradiated materials in a ho- cell environment. Due to the challenges of implementing a PST test in-cell, development efforts included sample preparation of double-edge notched specimens using a specific holder and a mill and a hot-cell compatible fixture design.

Out-cell MBT and in-cell PST test capabilities enable the preselection of cladding candidates based on failure strains and expected safety limits. Both tests can also inform future experiments on ATF candidates at the US Department of Energy's Transient Reactor Test Facility. Thus, unirradiated FeCrAl testing will be performed using PST tests in current FY. The obtained data from PST will be compared with the results of MBT. After these tests, PST fixture is expected to be installed in the hot-cell for future irradiated cladding tests.

5. REFERENCES

[1] T. Sugiyama, M. Umeda, T. Fuketa, H. Sasajima, Y. Udagawa, F. Nagase, Failure of high burnup fuels under reactivity-initiated accident conditions, Ann. Nucl. Energy. 36 (2009) 380–385. doi:10.1016/j.anucene.2008.12.003.

[2] J. Papin, B. Cazalis, J.M. Frizonnet, J. Desquines, F. Lemoine, V. Georgenthum, F. Lamare, M. Petit, Summary and interpretation of the CABRI REP-Na program, Nucl. Technol. 157 (2007) 230–250.

[3] B. Cazalis, J. Desquines, S. Carassou, T. Le Jolu, C. Bernaudat, T. Le Jolu, C. Bernaudat, The plane strain tests in the PROMETRA program, J. Nucl. Mater. 472 (2016) 127–142. doi:10.1016/j.jnucmat.2016.01.023.

[4] S. Leclercq, A. Parrot, M. Leroy, Failure characteristics of cladding tubes under RIA conditions, Nucl. Eng. Des. 238 (2008) 2206–2218. doi:10.1016/j.nucengdes.2008.03.017.

[5] M.N. Cinbiz, N. Brown, R.R. Lowden, M.N. Gussev, K.D. Linton, K.A. Terrani, Report on Design and Failure Limits of SiC/SiC and FeCrAl ATF Cladding Concepts under RIA, Oak Ridge, TN (United States), 2018. doi:10.2172/1461053.

[6] T.M. Link, D.A. Koss, A.T. Motta, Failure of Zircaloy cladding under transverse plane-strain deformation, Nucl. Eng. Des. 186 (1998) 379–394.

[7] K.G. Field, M.A. Snead, Y. Yamamoto, K.A. Terrani, ORNL/TM-2017/186 Rev.1 Handbook of FeCrAl Alloys for Nuclear Power Production Applications, Oak Ridge, TN (United States), 2017.

[8] Y. Yamamoto, B.A. Pint, K.A. Terrani, K.G. Field, Y. Yang, L.L. Snead, Development and property evaluation of nuclear grade wrought FeCrAl fuel cladding for light water reactors, J. Nucl. Mater. 467 (2015) 703–716. doi:10.1016/j.jnucmat.2015.10.019.

[9] M.N. Cinbiz, N.R. Brown, K.A. Terrani, R.R. Lowden, D. Erdman, A pulse-controlled modified-burst test instrument for accident-tolerant fuel cladding, Ann. Nucl. Energy. 109 (2017) 396–404. doi:10.1016/j.anucene.2017.05.058.

[10] M.A. Martin-Rengel, F.J. Gómez Sánchez, J. Ruiz-Hervías, L. Caballero, Determination of the hoop fracture properties of unirradiated hydrogen-charged nuclear fuel cladding from ring compression tests, J. Nucl. Mater. (n.d.). doi:http://dx.doi.org/10.1016/j.jnucmat.2013.01.311.

[11] M. Le Saux, J. Besson, S. Carassou, C. Poussard, X. Averty, Behavior and failure of uniformly hydrided Zircaloy-4 fuel claddings between 25 °C and 480 °C under various stress states, including RIA loading conditions, Eng. Fail. Anal. 17 (2010) 683–700. doi:10.1016/j.engfailanal.2009.07.001.